Received: 28 February 2022 | Revised: 02 April 2022 | Accepted: 02 April 2022
DOI: 10.22034/ecc.2022.335450.1392
Eurasian Chemical Communications
SAMI

FULL PAPER

New fused-coumarin composites: synthesis, anticancer and antioxidant potentials evaluation

Sara Firas Jasim* | **Yasser Fakri Mustafa**

Pharmaceutical Chemistry Department, College of Pharmacy, University of Mosul, Mosul, Iraq

Today, there is a pressing need to develop anti-carcinogenic and anti-oxidative agents with the improved potency and fewer side effects. To this end, new coumarin composites were prepared through the Pechmann condensation reaction. The skeletal formulas of the prepared composites were elucidated via well-known spectroscopical methods, whereas the pharmacokinetics and drug-likeness of them were analyzed by the ADME study. The MTT-based test was employed to estimate the effect of the prepared coumarin composites as neoplastic inhibitory agents *in-vitro* towards six cancerous-cell lines involving AMN3, SKG, KYSE-30, HeLa, SK-OV-3, and MCF-7. Additionally, the previous test was utilized to inspect the safety of the prepared composites towards a normal human-cell line. Likewise, the prepared coumarin composites' anti-oxidative effect was investigated *in-vitro* by utilizing DPPH and hydroxide radical moieties. The findings unveiled that the composite with the powerful electronegative substituent, **SF4**, had an eminent neoplastic inhibitory effect among other composites, with IC_{50} values close to the gold standard (5-fluorouracil), specifically towards HeLa and MCF-7 cells. Concerning safety, when compared with the standard, the prepared coumarin composites had a higher safety level on the inspected normal-cell line. Among them, the composite **SF4** had the highest safety rating. Moreover, composite **SF0** demonstrated a remarkable antioxidative effect on the inspected free radical moieties, with TC_{50} values near the standard (cevitamic acid). Also, most prepared composites had appropriate hypothetical pharmacokinetics and drug-likeness based on the ADME analysis, indicating that they could be used by the oral route.

KEYWORDS

Coumarin composites; anticancer; antioxidant; ADME; normal cells.

***Corresponding Author:**
Sara Firas Jasim
Email:
sara.20php6@student.uomosul.edu.iq
Tel.: +9647722283818

Introduction

Cancer is a serious global concern. It refers to a group of diseases in which cells grow out of control and can infiltrate the other organs or be dispersed all over the body. In terms of mortality and morbidity, it is a fatal disease which ranks second only to heart and blood vessel diseases [1]. According to the World Health Organization, cancerous diseases affect one out of every six women and one out of every five men at some point in their lives [2]. It is worth mentioning that documented registries of mortality and incidence have not decreased in recent years, and regrettably, cancer is expected to continue as the leading cause of death in the upcoming years [3]. Even though cancerous research has resulted in some novel and efficacious resolutions, the medications utilized as therapies have

obvious practical issues involving low specificity, fatal side effects, and cancerous multidrug resistance. The discovery of new neoplastic inhibitory agents with potency, safety, and selectivity characteristics is an enormous priority right now, both scientifically and commercially [4,5].

In biological systems, oxidative stress is a complex state in which the formation of free radical moieties is ungovernable and the body's capacity to trap and eradicate these reactive moieties via endogenous and exogenous antioxidative mechanisms is insufficient [6]. According to several studies conducted on humans, a fierce link has been found between the oxidative stress and the onset or development of many illnesses such as cancer, diabetes mellitus, cardiovascular disease, and the others. These findings highlight the importance of striking an optimal balance between free reactive moieties and antioxidants to prevent the consequential physiological and pathological impacts [7]. The antioxidants are considered remedial for the harm caused by these free damaging moieties. Nonetheless, due to severe side effects and low efficacy, just a small number of antioxidants have been authorized for use clinically to date. Consequently, novel and more efficient antioxidants with minimal side effects are urgently needed [8].

The coumarins are members of a large hetero-aromatic family [9]. They are intriguing molecules for many fields of study due to the conjugated systems found in their fused rings [10]. Coumarin compounds are used in industry as additives in food and as ingredients in perfumes and cosmetics. However, its most important usage is to synthesize different products in the pharmaceutical industry [11]. Coumarins, from natural and/or synthetic sources, have different biomedical potentials, such as anti-diabetic, anti-viral, anti-tubercular, anti-fungal, anti-coagulant, anti-cancer, anti-bacterial, and anti-oxidant [12] properties. Moreover, these molecules have many appealing characteristics such as low toxicity, high bioavailability, simple structure, and low molecular weight which confirm that they could play a significant role in drug development and research [13].

Benzocoumarins, also known as benzochromenones, are a prime bioactive fused-coumarin class. In the past few years, numerous researchers have concentrated their endeavors on isolating, synthesizing, and studying the bioactivities of these coumarin-based compounds due mainly to their expander system of π-conjugation compared to coumarins [14]. These studies revealed that the compounds with a benzocoumarin core have various biomedical properties including anti-diabetic, anti-microbial, anti-cancer, anti-oxidant, and anti-dyslipidemic activities [15]. The anti-carcinogenic and anti-oxidative properties have taken precedence among the examined activities. As a result, benzocoumarins may be useful as scaffolds for promising neoplastic inhibitory and antioxidative agents [16].

This work aims to prepare new tri-substituted coumarin composites. An ADME study was performed utilizing a preADMET predictor, an online server to analyze the pharmacokinetic parameters and drug-likeness of the prepared coumarin composites. The neoplastic inhibitory effect of the prepared composites was screened *in-vitro* by employing an MTT-based test towards six cancerous-cell lines involving AMN3, SKG, KYSE-30, HeLa, SK-OV-3, and MCF-7. Moreover, to determine their safety, the toxicity of our composites towards a normal-cell line was also checked. The latter investigation was conducted by measuring the cytotoxic effect of the composites on human normal prostate epithelial cells (RWPE-1). Besides, the antioxidative effect of the prepared coumarin composites was screened *in-vitro* by utilizing DPPH and hydroxide radicals which were used to assess

the prepared composites' capacity to trap free radical moieties.

Resources and procedures

Devices and chemicals

Chemical compounds, solvents, and reagents used to prepare coumarin composites, as well as the biological evaluation systems, were procured from some international resources such as Haihang, Bioworld, Chem-Lab, Labcorp, Sigma-Aldrich, Scharlau, and the others. The procured chemical and biological agents were employed directly without further purification. An ultrasonic-water bath (40 kHz, 350 W, Power Sonic410, Korea) was operated as a sonication system. A digital electrothermal apparatus (CIA9300) was utilized to measure the melting temperatures (Mp) of the prepared coumarin composites without pre-correction via an open-capillary approach. The synthesis status progression was checked, and the prepared composites' purity was determined using thin-layer chromatography (TLC). An aluminum-based silica gel sheet (F254) and a mixture of chloroform: MeOH (4:1) served as the fixed and moveable phases in this technique. In addition, spectrometers involved Bruker Avance DRX-300 MHz, Bruker-α- ATR-FTIR, and UV-1600PC UV-Vis were operated to record the prepared coumarin composites spectra of ^{13}C- and ^{1}H-NMR, FTIR, and UV, respectively.

Chemical pathway

Synthesis of composite SF0

At room temperature (RT), 6-amino-7-chloronaphthalen-2-ol (1.930 g, 10.00 mmol) and nitric acid sodium salt (3.450 g, 50.00 mmol) were mixed and stirred for 15 minutes in 90.00 mL of MeOH. At that temperature, 11.50 mL of ethanoic acid was slowly added to the resultant solution, and the stirring was continued strenuously for 6 hours. The gathered solid product was re-crystalized from an aqueous EtOH solution after vaporizing the solvent, as indicated in Equation 1 [17].

6-Amino-7-chloronaphthalen-2-ol — SF0

EQUATION 1 The synthesis of SF0 from 6-amino-7-chloronaphthalen-2-ol

7-Chloro-6-methoxynaphthalen-2-ol (**SF0**): French pink; Yield= 43% (0.89 g); Mp= 160-162°C; R_f = 0.23; λ_{max} (EtOH)= 517 nm; IR ν_{max} (cm^{-1}): 3300 (br, phenolic O-H), 3076 (m, aromatic C-H), 2957 (w, alkyl C-H), 1561 (s, aromatic C=C), 1281, 1073 (s, ether C-O-C), 916 (s, C-Cl); ^{1}H-NMR (ppm, 300 MHz, DMSO-d_6): δ= 8.08 (1H, d, *J*= 9 Hz, 4-H), 7.62 (1H, s, 8-H), 7.48 (1H, s, 1-H), 7.33 (1H, s, 5-H), 7.22 (1H, d, *J*= 9 Hz, 3-H), 5.56 (1H, s, 2-OH), 4.02 (3H, s, 6-OCH_3); ^{13}C-NMR (ppm, 75 MHz, DMSO-d_6): δ= 157.1 (C, C-6), 155.7 (C, C-2), 133.1 (C, C-9), 131.4 (CH, C-4), 129.8 (C, C-10), 128.5 (CH, C-8), 126.9 (C, C-7), 120.2 (CH, C-3), 111.4 (CH, C-1), 108.6 (CH, C-5), and 50.1 (CH_3, OCH_3-6).

Synthesis of composite SF1

Method A

With the assistance of heating, **SF0** (2.750 g, 13.18 mmol) was dissolved in acetone

dicarboxylic acid (3.50 mL, 15.00 mmol). After that, the resulting solution was dropped very slowly from a separatory funnel into 25.00 mL of precooled concentrated H_2SO_4 submerged in an ice bath. During the addition, the reaction mixture was stirred, and the temperature was kept under 10.0 °C. The reaction mixture was then retained at RT for 20 hours with continuous stirring before being shed over the ice/water combination. The precipitate was filtered off and rinsed well with cooled water, as illustrated in the upper route in Equation 2 [18].

Method B

With the assistance of heating, **SF0** (2.750 g, 13.18 mmol) was dissolved in acetone dicarboxylic acid (3.50 mL, 15.00 mmol). After that, the resulting solution was dropped very slowly from a separatory funnel into 25.00 mL of precooled concentrated H_2SO_4 submerged in in an ice bath. During the addition, the reaction mixture was stirred, and the temperature was kept under 10.0 °C. Then, the reaction mixture was settled under sonication for 1.5 hours at 30.0 °C before being shed over an ice/water mixture. The precipitate was filtered off and purified by washing with cooled water, as demonstrated in the lower route in Equation 2 [19].

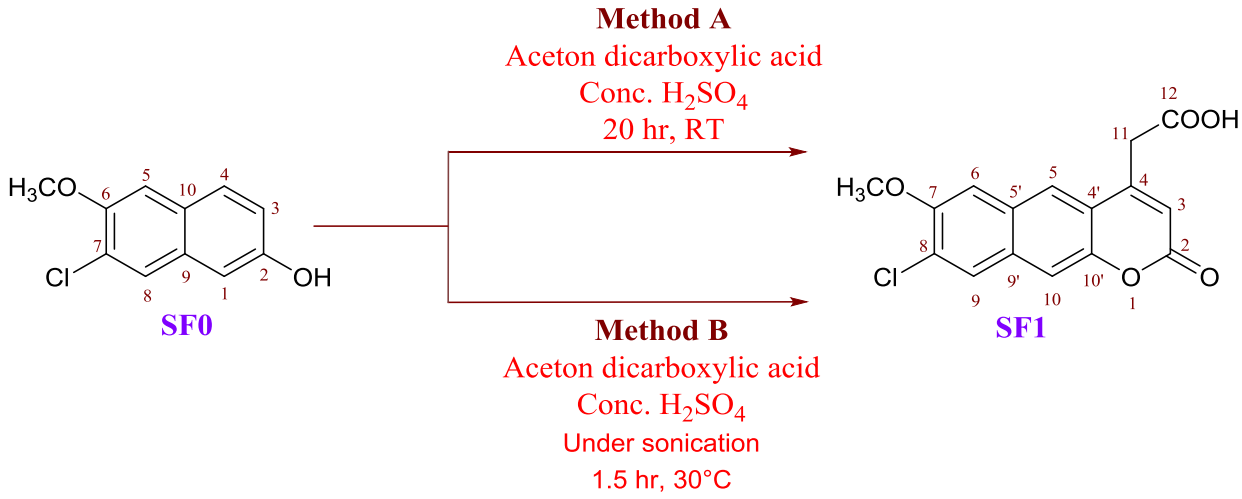

EQUATION 2 The synthesis of SF1 from SF0 through the Pechmann reaction

11-(8-Chloro-7-methoxy-2-oxo-2*H*-benzo[*g*]chromen-4-yl)acetic acid (**SF1**): Yellowish powder; Yield= 79.76% (3.35 g in method A) and 88.09% (3.70 g in method B); Mp= 186-188°C; R_f = 0.19; λ_{max} (EtOH)= 467 nm; IR ν_{max} (cm^{-1}): 3062 (w, *cis*-alkene C-H), 3015 (br, carboxylic acid O-H), 2957 (w, methoxy C-H), 2891 (w, alkyl C-H), 1734 (s, lactonic ester C=O), 1692 (s, carboxylic acid C=O), 1590 (s, *cis*-alkene C=C), 1548 (m, aromatic C=C), 1247, 1046 (s, ether C-O-C), 941 (s, C-Cl); ^{1}H-NMR (ppm, 300 MHz, DMSO-d_6): δ= 11.09 (1H, s, 12-OH), 7.92 (1H, s, 5-H), 7.60 (1H, s, 9-H), 7.43 (1H, s, 6-H), 7.12 (1H, s, 10-H), 6.35 (1H, s, 3-H), 4.03 (3H, s, 7-OCH_3), 3.12 (2H, s, 11-H); ^{13}C-NMR (ppm, 75 MHz, DMSO-d_6): δ= 173.1 (C, C-12), 162.2 (C, C-2), 154.4 (C, C-7), 153.0 (C, C-4), 151.8 (C, C-10'), 130.2 (C, C-9'), 128.1 (C, C-5'), 127.5 (C, C-4'), 126.4 (CH, C-9), 125.1 (CH, C-5), 124.5 (C, C-8), 115.8 (CH, C-3), 113.4 (CH, C-10), 109.4 (CH, C-6), 50.1 (CH_3, OCH_3-7), and 30.9 (CH_2, C-11).

Synthesis of composites SF2-SF7

Composite **SF1** (1.593 g, 5.00 mmol) was added to refreshed $SOCl_2$ (25.00 mL) in a twin-neck flask and submerged in a salted ice bath. A condenser fitted the middle neck, whereas a plug furnished with blue litmus-

paper plugged the other. In moisture-less environment, the mixture was stirred gently for a half-hour, then at RT for another half-hour. This was followed by 3 hours of refluxing. The reaction progression was tracked by the litmus-paper color change, which was renewed every half-hour. The distillation of $SOCl_2$ excess when the litmus paper blue color remained unchanged gave the alkanoyl chloride intermediate in the flask bottom as a solid white product [3].

At RT, a solution of phenolic-based derivative (4.80 mmol) and azabenzene (1.00 mL) in 50.00 mL of anhydrous ethoxyethane was poured into the same flask housing the white crude. The mixture was agitated for a half-hour in moisture-less environment. According to the change in litmus-paper color, the reaction was refluxed for a time, as mentioned previously. Then, 50.00 mL of water was added to the mixture when the reaction was completed, followed by separating, dehydrating, and evaporating the organic layer. From a CH_2Cl_2: dimethylketone (2:1) mixture, the derivatives of **SF1** were recrystallized, as described in Equation 3 [3].

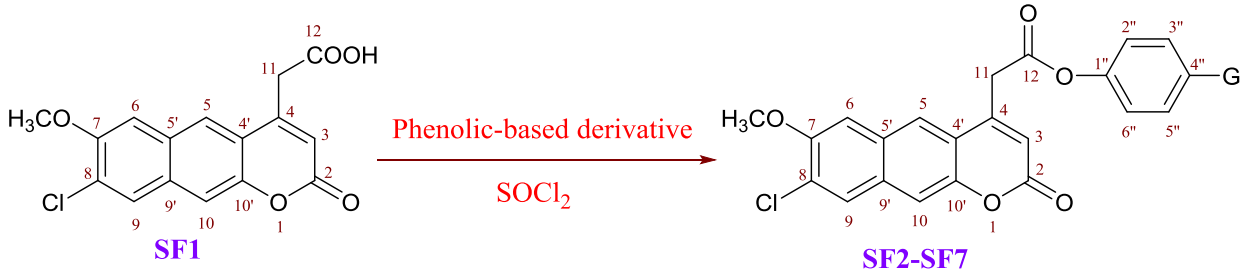

SF2: G= OCH_3; **SF3**: G= CH_3; **SF4**: G= F;
SF5: G= Cl; **SF6**: G= Br; **SF7**: G= I

EQUATION 3 The synthesis of SF2-SF7 composites from SF1

4''-Methoxyphenyl 11-(8-chloro-7-methoxy-2-oxo-2*H*-benzo[*g*]chromen-4-yl)acetate (**SF2**): White powder; Yield= 76.27% (1.62 g); Mp= 171-173°C; R_f = 0.63; λ_{max} (EtOH)= 331 nm; IR ν_{max} (cm^{-1}): 3096 (m, *cis*-alkene C-H), 2917 (m, methoxy C-H), 2821 (w, alkyl C-H), 1731 (s, lactonic ester C=O), 1710 (s, ester C=O), 1665 (s, *cis*-alkene C=C), 1595 (s, aromatic C=C), 1266, 1028 (s, ether C-O-C), 985 (s, C-Cl); ^{1}H-NMR (ppm, 300 MHz, DMSO-d_6): δ= 7.92 (1H, s, 5-H), 7.60 (1H, s, 9-H), 7.43 (1H, s, 6-H), 7.12 (1H, s, 10-H), 7.01 (2H, d, *J*= 6 Hz, 3''-, 5''-H), 6.74 (2H, d, *J*= 6 Hz, 2''-, 6''-H), 6.35 (1H, s, 3-H), 4.12 (3H, s, 4''-OCH_3), 4.03 (3H, s, 7-OCH_3), 3.12 (2H, s, 11-H); ^{13}C-NMR (ppm, 75 MHz, DMSO-d_6): δ= 169.5 (C, C-12), 162.2 (C, C-2), 156.4 (C, C-4''), 154.4 (C, C-7), 153.0 (C, C-4), 151.8 (C, C-10'), 144.6 (C, C-1''), 130.2 (C, C-9'), 128.1 (C, C-5'), 127.5 (C, C-4'), 126.4 (CH, C-9), 125.1 (CH, C-5), 124.5 (C, C-8), 120.1 (CH, C-3'', -5''), 115.8 (CH, C-3), 113.4 (CH, C-10), 112.3 (CH, C-2'', -6''), 109.4 (CH, C-6), 51.1 (CH_3, OCH_3-4''), 50.1 (CH_3, OCH_3-7), and 28.3 (CH_2, C-11).

4''-Tolyl 11-(8-chloro-7-methoxy-2-oxo-2*H*-benzo[*g*]chromen-4-yl)acetate (**SF3**): Off-white powder; Yield= 74.36% (1.52 g); Mp= 156-158°C; R_f = 0.58; λ_{max} (EtOH)= 378 nm; IR ν_{max} (cm^{-1}): 3090 (m, *cis*-alkene C-H), 2912 (w, methoxy C-H), 2819 (w, alkyl C-H), 1733 (s, lactonic ester C=O), 1713 (s, ester C=O), 1668 (s, *cis*-alkene C=C), 1597 (s, aromatic C=C), 1267, 1030 (s, ether C-O-C), 985 (s, C-Cl); ^{1}H-NMR (ppm, 300 MHz, DMSO-d_6): δ= 7.92 (1H, s, 5-H), 7.60 (1H, s, 9-H), 7.43 (1H, s, 6-H), 7.25 (2H, d, *J*= 6 Hz, 3''-, 5''-H), 7.12 (1H, s, 10-H), 7.02 (2H, d, *J*= 6 Hz, 2''-, 6''-H), 6.35 (1H, s, 3-H), 4.02 (3H, s, 7-OCH_3), 3.12 (2H, s, 11-H), 2.75 (3H, s, 4''-CH_3); ^{13}C-NMR (ppm, 75 MHz, DMSO-d_6): δ= 169.5 (C, C-12), 162.2 (C, C-2), 154.4 (C, C-7), 153.0 (C, C-4), 151.8 (C, C-10'), 149.3 (C, C-1''), 134.2 (C, C-4''), 130.2 (C, C-9'), 128.1 (C, C-5'), 127.5 (C, C-4'), 126.4 (CH, C-9), 125.1 (CH, C-5),

124.5 (C, C-8), 122.0 (CH, C-3'', -5''), 119.0 (CH, C-2'', -6''), 115.8 (CH, C-3), 113.4 (CH, C-10), 109.4 (CH, C-6), 50.1 (CH_3, OCH_3-7), 27.5 (CH_2, C-11), and 24.1 (CH_3, CH_3-4'').

4''-Fluorophenyl 11-(8-chloro-7-methoxy-2-oxo-2*H*-benzo[*g*]chromen-4-yl)acetate (**SF4**): White powder; Yield= 69.28% (1.43 g); Mp= 166-168°C; R_f = 0.42; λ_{max} (EtOH)= 330 nm; IR ν_{max} (cm^{-1}): 3070 (m, *cis*-alkene C-H), 2918 (w, methoxy C-H), 2820 (w, alkyl C-H), 1733 (s, lactonic ester C=O), 1711 (s, ester C=O), 1666 (s, *cis*-alkene C=C), 1597 (s, aromatic C=C), 1266, 1028 (s, ether C-O-C), 1077 (s, C-F), 986 (s, C-Cl); ^{1}H-NMR (ppm, 300 MHz, DMSO-d_6): δ= 7.92 (1H, s, 5-H), 7.60 (1H, s, 9-H), 7.43 (1H, s, 6-H), 7.26 (2H, d, *J*= 6 Hz, 2''-, 6''-H), 7.12 (1H, s, 10-H), 7.04 (2H, d, *J*= 6 Hz, 3''-, 5''-H), 6.35 (1H, s, 3-H), 4.02 (3H, s, 7-OCH_3), 3.12 (2H, s, 11-H); ^{13}C-NMR (ppm, 75 MHz, DMSO-d_6): δ= 169.5 (C, C-12), 162.2 (C, C-2), 158.7 (C, C-4''), 154.4 (C, C-7), 153.0 (C, C-4), 151.8 (C, C-10'), 147.9 (C, C-1''), 130.2 (C, C-9'), 128.1 (C, C-5'), 127.5 (C, C-4'), 126.4 (CH, C-9), 125.1 (CH, C-5), 124.5 (C, C-8), 120.7 (CH, C-2'', -6''), 115.8 (CH, C-3), 113.4 (CH, C-10), 109.4 (CH, C-6), 108.5 (CH, C-3'', -5''), 50.1 (CH_3, OCH_3-7), and 27.5 (CH_2, C-11).

4''-Chlorophenyl 11-(8-chloro-7-methoxy-2-oxo-2*H*-benzo[*g*]chromen-4-yl)acetate (**SF5**): White powder; Yield= 68.50% (1.47 g); Mp= 158-160°C; R_f = 0.46; λ_{max} (EtOH)= 341 nm; IR ν_{max} (cm^{-1}): 3068 (m, *cis*-alkene C-H), 2916 (w, methoxy C-H), 2820 (w, alkyl C-H), 1730 (s, lactonic ester C=O), 1710 (s, ester C=O), 1667 (s, *cis*-alkene C=C), 1595 (s, aromatic C=C), 1265, 1031 (s, ether C-O-C), 985 (s, C-Cl); ^{1}H-NMR (ppm, 300 MHz, DMSO-d_6): δ= 7.92 (1H, s, 5-H), 7.60 (1H, s, 9-H), 7.53 (2H, d, *J*= 6 Hz, 3''-, 5''-H), 7.43 (1H, s, 6-H), 7.35 (2H, d, *J*= 6 Hz, 2''-, 6''-H), 7.12 (1H, s, 10-H), 6.35 (1H, s, 3-H), 4.02 (3H, s, 7-OCH_3), 3.12 (2H, s, 11-H); ^{13}C-NMR (ppm, 75 MHz, DMSO-d_6): δ= 169.5 (C, C-12), 162.2 (C, C-2), 154.4 (C, C-7), 153.0 (C, C-4), 151.8 (C, C-10'), 150.4 (C, C-1''), 132.0 (C, C-4''), 130.2 (C, C-9'), 128.1 (C, C-5'), 127.5 (C, C-4'), 126.4 (CH, C-9), 125.1 (CH, C-5), 124.5 (C, C-8), 122.9 (CH, C-3'', -5''), 120.5 (CH, C-2'', -6''), 115.8 (CH, C-3), 113.4 (CH, C-10), 109.4 (CH, C-6), 50.1 (CH_3, OCH_3-7), and 33.2 (CH_2, C-11).

4''-Bromophenyl 11-(8-chloro-7-methoxy-2-oxo-2*H*-benzo[*g*]chromen-4-yl)acetate (**SF6**): White powder; Yield= 62.50% (1.48 g); Mp= 142-144°C; R_f = 0.49; λ_{max} (EtOH)= 335 nm; IR ν_{max} (cm^{-1}): 3066 (m, *cis*-alkene C-H), 2913 (w, methoxy C-H), 2819 (w, alkyl C-H), 1732 (s, lactonic ester C=O), 1709 (s, ester C=O), 1664 (s, *cis*-alkene C=C), 1593 (s, aromatic C=C), 1262, 1023 (s, ether C-O-C), 986 (s, C-Cl), 900 (s, C-Br); ^{1}H-NMR (ppm, 300 MHz, DMSO-d_6): δ= 7.92 (1H, s, 5-H), 7.77 (2H, d, *J*= 6 Hz, 3''-, 5''-H), 7.60 (1H, s, 9-H), 7.43 (1H, s, 6-H), 7.11 (1H, s, 10-H), 6.95 (2H, d, *J*= 6 Hz, 2''-, 6''-H), 6.35 (1H, s, 3-H), 4.02 (3H, s, 7-OCH_3), 3.13 (2H, s, 11-H); ^{13}C-NMR (ppm, 75 MHz, DMSO-d_6): δ= 169.5 (C, C-12), 162.2 (C, C-2), 154.4 (C, C-7), 153.0 (C, C-4), 151.8 (C, C-10'), 151.3 (C, C-1''), 130.2 (C, C-9'), 128.1 (C, C-5'), 127.5 (C, C-4'), 126.4 (CH, C-9), 125.1 (CH, C-5), 124.5 (C, C-8), 123.6 (CH, C-3'', -5''), 121.3 (CH, C-2'', -6''), 118.5 (C, C-4''), 115.8 (CH, C-3), 113.4 (CH, C-10), 109.4 (CH, C-6), 50.1 (CH_3, OCH_3-7), and 33.2 (CH_2, C-11).

4''-Iodophenyl 11-(8-chloro-7-methoxy-2-oxo-2*H*-benzo[*g*]chromen-4-yl)acetate (**SF7**): White powder; Yield= 64.54% (1.68 g); Mp= 136-138°C; R_f = 0.51; λ_{max} (EtOH)= 339 nm; IR ν_{max} (cm^{-1}): 3064 (m, *cis*-alkene C-H), 2913 (w, methoxy C-H), 2823 (w, alkyl C-H), 1733 (s, lactonic ester C=O), 1711 (s, ester C=O), 1661 (s, *cis*-alkene C=C), 1592 (s, aromatic C=C), 1265, 1028 (s, ether C-O-C), 986 (s, C-Cl), 866 (s, C-I); ^{1}H-NMR (ppm, 300 MHz, DMSO-d_6): δ= 7.92 (1H, s, 5-H), 7.85 (2H, d, *J*= 6 Hz, 3''-, 5''-H), 7.60 (1H, s, 9-H), 7.43 (1H, s, 6-H), 7.11 (1H, s, 10-H), 6.83 (2H, d, *J*= 6 Hz, 2''-, 6''-H), 6.35 (1H, s, 3-H), 4.00 (3H, s, 7-OCH_3), 3.13 (2H, s, 11-H); ^{13}C-NMR (ppm, 75 MHz, DMSO-d_6): δ= 169.5 (C, C-12), 162.2 (C, C-2), 154.4 (C, C-7), 153.0 (C, C-4), 151.8 (C, C-10'), 151.2 (C, C-1''), 130.2 (C, C-9'), 129.6 (CH, C-3'', -5''), 128.1 (C, C-5'),

127.5 (C, C-4'), 126.4 (CH, C-9), 125.1 (CH, C-5), 124.5 (C, C-8), 120.7 (CH, C-2'', -6''), 115.8 (CH, C-3), 113.4 (CH, C-10), 109.4 (CH, C-6), 93.0 (C, C-4''), 50.2 (CH_3, OCH_3-7), and 33.2 (CH_2, C-11).

Assessment of the bioactivities

Neoplastic inhibitory effect

In DMSO, the prepared coumarin composites, along with the standard 5-fluorouracil (5-FUra), were dissolved to obtain seven diluted concentrations in a doubly serial manner, with orders between 400.00 and 6.25 µg/mL. Then, in a 96-well format, 10^4 cells of the inspected cancerous-line were loaded over a growth-enhanced medium in each well and proliferated for 24 hours. After that, every well was exposed separately with one of the previously prepared concentrations. Following 72 hours of exposure, the MTT color reagent (28.0 µL, 3.270 mM) was laid to check the viability of cells after the growth-enhanced medium was discarded. Then, the cells were harbored for an additional 1.5 hours at 37.0 °C. The absorbance of every well was measured using a microplate reader calibrated at 492.0 nm. The absorbance readings of the unexposed and exposed wells were symbolized by Abs_{ue} and Abs_e, respectively. Each inspected coumarin composite's neoplastic inhibitory effect was represented as a growth repression percent (GR%) equivalent to $(Abs_{ue}-Abs_e/Abs_{ue}) \times 100$. In nonlinear regression, the GR% values were plotted against the logarithmic concentrations to calculate the IC_{50} score. For each inspected coumarin composite, the result optimization was achieved by triplicating the procedure steps [20].

Free-radicals trapping effect

Exploiting Vit.C as a standard, the prepared coumarin composites' capacities to transmit an electron in the oxido-reduction reaction and trap the hydroxide and DPPH (2,2-diphenyl-1-picryl-hydrazyl) radicals were estimated. From a master solution (1.00 mg/mL), seven sub-master solutions in a doubly diluted serial manner, with orders between 400.00 and 6.25 µg/mL, were acquired using EtOH as a thinner. Each inspected composite's anti-oxidative effect was represented as a trapping percent (T%) equivalent to $(Abs_{cev} - Abs_{test}/Abs_{cev}) \times 100$. The absorbance readings for the Vit.C and the inspected composite were symbolized by Abs_{cev} and Abs_{test}, respectively. In nonlinear regression, the TC% values were plotted against the logarithmic concentrations to calculate the TC_{50} score. The latter expresses the concentration at which half of the ferric ions or free radical moieties are reduced or trapped, respectively, by Vit.C or prepared coumarin composites [21].

DPPH-radical trapping test

In the beginning, 0.50 mL of 0.10 mM alcoholic DPPH solution was pipetted into 1.50 mL of the inspected solution at a definite concentration to make the testing combination. After that, the combination was harbored for 0.5 hours at 25.0 °C while being kept out of light by an aluminum shield. At 517.0 nm, the resultant solution's capacity to exterminate the violet color of DPPH was estimated colorimetrically. An alcoholic DPPH solution (0.50 mL) was added to EtOH (1.50 mL) to obtain the blank solution [22].

Hydroxide-radical trapping test

First, 2.40 mL of a buffer solution of potassium phosphate (pH 7.8, 0.20 M) was pipetted to 1.50 mL of the inspected solution at a definite concentration. Following that, a trichloroiron (60.0 µL, 0.0010 M), 1,10-phenanthroline (90.0 µL of 0.0010 M), and superoxol (150.0 µL of 0.170 M) were pipetted to the previous combination. At 560.0 nm, the solution's trapping capacity was estimated colorimetrically after

harboring for 5 minutes at 25.0 °C. This test's blank solution included all of the preceding additions, with the exception of the inspected solution, which was substituted by the buffer solution [23].

Computer-based pharmacokinetic properties (ADME)

The ADME (absorption, distribution, metabolism, and excretion) and drug-likeness of the prepared coumarin composites were analyzed utilizing the preADMET predictor server, which depends on the two-dimensional skeletal formula of the inspected composites [24].

Results and discussion

Designing the synthetic pathway

As illustrated in Equations 1, 2, and 3, the design and synthesis of coumarin composites involved several steps. These steps begin with the aromatic nucleophilic substitution reaction by forming a diazonium salt intermediate at the C-6 position of 6-amino-7-chloronaphthalen-2-ol utilizing nitric acid sodium salt, MeOH, and ethanoic acid to produce **SF0**. It is noteworthy that this reaction is novel and was used for the first time here to substitute the amino group in the aromatic ring with the methoxy group [39]. Then, by applying two methods based on the Pechmann reaction, a coumarin composite **SF1** was prepared. The classic Pechmann reaction was chosen for the synthesis of this composite because of the starting material's generality, the availability, and the product's high yield [25].

In method A, the 2-naphthol composite **SF0** was condensed with acetone dicarboxylic acid, affording the tri-substituted coumarin composite **SF1** in a good yield of 79.76% by using concentrated H_2SO_4 as a catalyst at RT for 24 hours [40]. While in method B, the condensation of **SF0** with acetone dicarboxylic acid was achieved using concentrated H_2SO_4 as a catalyst to produce **SF1** with an excellent yield of 88.09% by employing an ultrasound bath for 1.5 hours at 30.0°C. It's important to mention that ultrasound-promoted reaction is a green method for chemical synthesis. Moreover, the sonication in method B reduced reaction time and increased the yield percentage [26].

Finally, the **SF1** carboxylic acid group was transformed by the $SOCl_2$ catalyst to prepare the acyl chloride-based intermediate. Then, different *para*-substituted phenolic compounds reacted with the generated intermediate to obtain the target composites (**SF2**-**SF7**) [3]. At the para position of the employed phenols, the group's nature impacted the yield percentage of the prepared composites. The good electron-donating group gave the most elevated percentage, whereas the good electron-withdrawing group gave the most decreased percentage. Spectroscopical data was used to affirm the structures of the prepared composites.

Computer-based pharmacokinetic evaluation

The analysis of the ADME profile of drug candidates is a significant constraint during drug discovery and lead compound selection. About 50 % of the candidates failed in the development stages due to unacceptable ADME profiles. To avoid this failure, *in-silico* technologies were successfully applied to predict ADME-related properties and provide guidance in the initial stages of drug discovery processes. Besides, studying these properties may aid in choosing the proper lead compounds before conducting *in-vitro* and *in-vivo* studies, which results in saving time and funds [27].

The assessment of the obtained results, as registered in Table 1, revealed a number of intriguing points. First of all, the prepared coumarin composites had excellent human intestinal absorption (HIA) in the range of (97.46–98.93%) and moderate Caco-2 cell

line permeability. These findings indicate that the absorption through the intestine might depend on other mechanisms besides passive diffusion. This is due to Caco-2 cell models' expression lacking certain transporters, mucus-secretory cells, and non-cellular parameters like bile acids and phospholipids that can also affect the absorption process. Further, tight junctions of the Caco-2 system make it less permeable to the composites that can be absorbed paracellularly [28].

Moreover, **SF2**-**SF7** composites inhibited the P-glycoprotein (P-gp) transporter. Hence, they can increase apical-to-basolateral intestinal permeability and bioavailability of drugs that are substrates for this efflux system. Also, the inhibition of the P-gp transporter can lead to several drug-drug interactions in the distribution and elimination processes [29]. In addition, the prepared coumarin composites except **SF1** inhibited the CYP3A4 enzyme which is responsible for metabolizing and eliminating about 50% of marketed drugs, so inhibiting this enzyme will result in a drug-drug interaction [30]. Further, the prepared composites inhibited the CYP2C9 enzyme, which may lead to drug-drug interactions with drugs which use this enzyme for their metabolism [59,60].

As well, all prepared composites except **SF0** had a high plasma protein binding capacity ranging between 89.46–100.00%, resulting in a low volume of distribution, a long plasma half-life, and a low clearance rate. High plasma protein binding capacity can also affect efficacy because only the free fraction of the drug is responsible for pharmacological activity [31]. Likewise, the prepared composites were non-permeable across the blood-brain barrier except **SF0**, which was permeable. Brain penetration is a critical factor considered when trying to avoid or target the brain during the designing step. Impermeability of composites in the blood-brain barrier reduces or eliminates the risk of undesirable CNS side effects and toxicity [32].

Finally, role-of-five comprises four physicochemical parameter requirements that determine drug-likeness for the oral delivery system, which involve H-bond acceptors ≤ 10, H-bond donors ≤ 5, a molecular mass ≤ 500.0, and log P ≤ 5.0. Generally, orally administered drugs should have no more than one break-up of these requirements to display good aqueous solubility and intestinal permeability profiles, or else absorption and bioavailability are likely to be poor. According to the *in-silico* study, all prepared composites except **SF0** complied with Lipinski's rule. As a result, these composites have lower attrition rates during drug development and clinical trials and thus have a better chance of reaching the market [33].

TABLE 1 In-silico-based pharmacokinetic profile of the prepared coumarin composites

Composite symbol	Role-of-five	BBB-P C.brain/C.blood	PPB %	CYP2C9 blockage	CYP2D6 blockage	CYP3A4 blockage	HIA %	Pgp blockage	Caco2-P nm/sec
SF0	Fit	2.19	19.94	Blocker	Nil	Blocker	97.71	Nil	32.85
SF1	Fit	0.010	89.46	Blocker	Nil	Nil	98.93	Nil	20.16
SF2	Fit	0.07	91.89	Blocker	Nil	Blocker	97.49	Blocker	34.99
SF3	Fit	0.16	92.88	Blocker	Nil	Blocker	97.50	Blocker	34.66
SF4	Fit	0.06	92.91	Blocker	Nil	Blocker	97.46	Blocker	34.80
SF5	Fit	0.08	93.94	Blocker	Nil	Blocker	97.69	Blocker	36.60
SF6	Fit	0.08	96.65	Blocker	Nil	Blocker	97.86	Blocker	34.61
SF7	Not-fit	0.09	100.00	Blocker	Nil	Blocker	98.42	Blocker	33.88

Role-of-five: Lipinski's rule, BBB-P: Blood-brain barrier penetration, PPB: Plasma protein binding, CYP2C9: Cytochrome-P450 2C9, CYP2D6: Cytochrome-P450 2D6, CYP3A4: Cytochrome-P450 3A4, HIA: Human intestinal absorption, Pgp: P-glycoprotein, Caco2-P: Caco2 cell permeability (human colorectal carcinoma).

Valuation of the bioactivities

Neoplastic inhibitory effect

The authoritative MTT-dye test protocol was applied to assess the prefatory neoplastic inhibitory effect of the pure prepared coumarin composites *in-vitro* towards six cancerous-cell lines. These cells comprised AMN3 (*murine mammary adenocarcinoma*, CVCL-M395), SKG (*human papillomavirus-related cervical squamous cell carcinoma*, C27676), KYSE-30 (*human Asian esophageal squamous cell carcinoma*, 94072011), HeLa (*epithelioid cervix carcinoma*, 93021013), SK-OV-3 (*Caucasian ovary adenocarcinoma*, 91091004), and MCF-7 (*Caucasian breast adenocarcinoma*, 86012803). The positive and negative dominions employed in the test were 5-FUra and DMSO, respectively.

According to the study's findings, indicated in Table 2, the prepared composites had a neoplastic inhibitory effect on inspected cancerous-cell lines but were less potent than 5-FUra, with IC_{50} values ranging between 13.08±1.05 µM and 100.02±1.16 µM. Also, the prepared composites revealed a similar pattern of a neoplastic inhibitory effect. The ranking of declining the neoplastic inhibitory effect matches with the order: **SF4**, **SF5**, **SF0**, **SF2**, **SF3**, **SF6**, **SF7**, and **SF1**. In comparison to other prepared composites, **SF4** exhibited a superior neoplastic inhibitory effect towards all the inspected cancerous-cell lines, with a potency close to 5-FUra, especially towards HeLa and MCF-7 cells. The authors attributed this remarkable impact to the presence of the fluoro group which was attached to position 4'' in the skeletal formula of **SF4**. Concerning a neoplastic inhibitory effect, numerous research articles emphasize the beneficial effect of fluoride substitution in the composite's aromatic system. In addition, as a hydrogen-bond acceptor, the fluoro group can participate in the interactions between the composite and the target [34]. On the other hand, the existence of a carboxylic acid moiety in the skeletal formula of composite **SF1** may be the reason for its lower neoplastic inhibitory effect compared to other prepared composites. From the author's perspective, the strong hydrophilic character of the carboxylic acid moiety in **SF1** increases hydrophilicity and decreases the penetration into cancerous-cells [35].

In contrast, the pure prepared coumarin composites were screened for cytotoxicity *in-vitro* towards a normal human-cell line (RWPE-1). Intriguingly, the findings listed in Table 2 revealed that the inspected composites had less cytotoxic impact compared to 5-FUra towards the inspected normal cells, with IC_{50} values ranging between 40.24±1.08 µM and 112.45±1.16 µM. The order of increasing the cytotoxic effect matches the following: **SF4**, **SF5**, **SF0**, **SF2**, **SF3**, **SF6**, **SF7**, and **SF1**. Composite **SF4** displayed the lowest cytotoxicity and the highest safety profile towards RWPE-1, among other prepared composites [36].

TABLE 2 The findings of the neoplastic inhibitory effect valuation concerning the prepared coumarin composites

Composite symbol	IC50 (µM) ± SD (n=3)						
	AMN3	SKG	KYSE-30	HeLa	SK-OV-3	MCF-7	RWPE-1
5-FUra	24.89±1.12	22.12±0.98	30.72±1.02	13.37±1.05	22.43±1.16	12.42±0.99	34.79±0.96
SF0	30.93±1.05	31.79±0.96	41.83±1.04	20.63±1.05	32.76±1.05	26.12±1.18	55.15±1.05
SF1	63.97±1.08	100.02±1.16	69.01±1.12	62.16±1.15	64.67±0.93	91.26±1.08	40.24±1.08
SF2	54.16±1.00	46.29±1.15	50.16±0.92	24.45±0.95	57.92±1.12	28.56±0.92	55.01±1.12
SF3	67.54±0.93	42.12±1.08	53.79±1.17	41.12±1.08	40.16±1.00	34.21±1.00	48.17±1.22
SF4	28.43±0.94	31.15±1.00	41.45±1.07	13.42±1.00	25.08±1.06	13.08±1.05	112.45±1.16
SF5	30.65±1.08	31.24±1.15	41.67±1.00	16.35±1.15	28.89±0.96	22.65±1.10	57.67±0.99
SF6	63.14±1.16	82.76±1.04	57.43±1.18	53.34±1.00	57.38±1.17	84.16±1.05	44.12±0.91
SF7	69.21±1.10	79.45±0.98	60.26±1.02	54.09±0.96	63.19±0.98	88.91±1.15	40.63±1.06

Free radicals trapping effect

The capacity of the pure prepared coumarin composites to trap the DPPH and hydroxide radical moieties *in-vitro* was monitored to evaluate their antioxidative effect. Based on findings revealed in Table 3, the prepared coumarin composites displayed a trapping effect towards the free damaging moieties but less than Vit.C, with TC_{50} values ranging between 46.12±1.20 µM and 112.01±0.96 µM. Also, the prepared composites exhibited a parallel pattern of trapping the two inspected radicals, which conformed to the following descending order: **SF0**, **SF2**, **SF3**, **SF1**, **SF5**, **SF6**, **SF4**, and **SF7**. This order indicates that as the conjugation system of the prepared composites was enhanced with electron-donating substituents, the antioxidative effect increased.

Composite **SF0** demonstrated a greater trapping impact on inspected radicals than other prepared composites, with potency comparable to that of Vit.C. The authors attributed this superior effect of **SF0** to the existence of the aromatic OH moiety at position 2 of its skeletal formula, which enhances the system's conjugation competence [8]. On the other hand, the lower antioxidative effect of **SF7**, **SF4**, **SF6**, and **SF5** compared to the other prepared composites may be due to the existence of halogen moieties at position 4'' of their skeletal formulas. From the author's perspective, these halogens weaken the system's conjugation competence as they are electron-withdrawing moieties [37-40].

TABLE 3 The findings of the antioxidative effect valuation concerning the prepared coumarin composites

Composite symbol	Test and Result	
	DPPH-radical trapping effect TC50 (µM) ± SD (n=3)	Hydroxide-radical trapping effect TC50 (µM) ± SD (n=3)
Vit.C	45.87 ± 1.12	50.73 ± 0.98
SF0	46.12 ± 1.20	56.76 ± 1.05
SF1	95.68 ± 1.15	94.89 ± 1.08
SF2	92.67 ± 1.15	89.14 ± 1.20
SF3	95.12 ± 0.99	92.37 ± 1.00
SF4	103.31 ± 1.05	106.10 ± 1.15
SF5	95.38 ± 1.10	101.06 ± 1.05
SF6	98.49 ± 1.08	101.52 ± 1.15
SF7	104.16 ± 1.14	112.01 ± 0.96

Conclusion

The objective of the present work was to prepare new tri-substituted coumarin composites and explore their neoplastic inhibitory and antioxidative effects *in-vitro*, as well. Besides, the safety of our prepared composites towards a normal human-cell line was screened. The research findings conceded that the prepared coumarin composites had a neoplastic inhibitory effect on the six inspected cancerous-cell lines, but less than the standard. The composite with the powerful electronegative substituent, **SF4**, demonstrated a prominent neoplastic inhibitory effect with potency proximate to the standard, particularly towards HeLa and MCF-7 cells. In term of safety, the prepared composites had a high safety profile on the inspected normal cells when compared to the standard. Among these composites, **SF4** indicated the highest level of safety. Also, in comparison to other composites, **SF0** displayed a marked antioxidative effect on the inspected free radical moieties, with potency close to the standard. Furthermore, nearly all prepared composites had suitable hypothetical pharmacokinetics and drug-

likeness for oral administration based on the *in-silico* study. Thus, they have a greater chance of reaching the market due to the lower exclusion rate in later stages of drug development.

Acknowledgements

The authors are praising the University of Mosul/College of Pharmacy for providing facilities that improved the quality of this work. The authors would also like to thank Dr. Sarah Ahmed Waheed, Dr. Rahma Mowaffaq Jebir, and Dr. Reem Nadher Ismael for their help regarding the literature search.

Ethical issues[1]

The scientific committee of the Pharmaceutical Chemistry Department was approved this work.

Competing interests

We have no conflicts of interest to disclose.

Authors' contributions

All authors contributed toward data analysis, drafting and revising the paper and agreed to responsible for all the aspects of this work.

Orcid:

Sara Firas Jasim:
https://www.orcid.org/0000-0002-7863-3313
Yasser Fakri Mustafa:
https://www.orcid.org/0000-0002-0926-7428

References

[1] K.V. Sashidhara, A. Kumar, M. Kumar, J. Sarkar, S. Sinha, *Bioorganic Med. Chem. Lett.,* **2010**, *20*, 7205–7211. [Crossref], [Google Scholar], [Publisher]

[2] L. Zhang, Z. Xu, *Eur. J. Med. Chem.,* **2019**, *181*, 111587. [Crossref], [Google Scholar], [Publisher]

[3] M.K. Bashir, Y.F. Mustafa, M.K. Oglah, *Period. Tche Quim.,* **2020**, *17*, 871–883. [Google Scholar], [Publisher]

[4] Y.F. Mustafa, *NeuroQuantology,* **2021**, *19*, 99–112. [Crossref], [Google Scholar], [Publisher]

[5] M.J. Ansari, S.A. Jasim, T.Z. Taban, D.O. Bokov, M.N. Shalaby, M.E. Al-Gazally, H.H. Kzar, M.T. Qasim, Y.F. Mustafa, M. Khatami, *J. Clust. Sci.,* **2022**, 4, 44–47. [Crossref], [Google Scholar], [Publisher]

[6] H. Sies, *Antioxidants,* **2020**, *9*, 852. [Crossref], [Google Scholar], [Publisher]

[7] R.R. Khalil, Y.F. Mustafa, *Syst. Rev. Pharm.,* **2020**, *11*, 57–63. [Pdf], [Google Scholar], [Publisher]

[8] M.K. Oglah, Y.F. Mustafa, M.K. Bashir, M.H. Jasim, *Syst. Rev. Pharm.,* **2020**, *11*, 472–481. [Google Scholar], [Publisher]

[9] Y.F. Mustafa, N.T. Abdulaziz, *Syst. Rev. Pharm.,* **2020**, *11*, 438–452. [Google Scholar], [Publisher]

[10] Y.F. Mustafa, R.R. Khalil, E.T. Mohammed, M.K. Bashir, M.K. Oglah, *Arch. Razi Inst.,* **2021**, *76*, 1297–1305. [Crossref], [Google Scholar], [Publisher]

[11] Y.F. Mustafa, *J. Glob. Pharma Technol.,* **2019**, *11*, 1–10. [Google Scholar], [Publisher]

[12] Y.F. Mustafa, R.R. Khalil, E.T. Mohammed, *Syst. Rev. Pharm.* **2020**, *11*, 382–387. [Google Scholar], [Publisher]

[13] E.T. Mohammed, Y.F. Mustafa, *Syst. Rev. Pharm.,* **2020**, *11*, 64–70. [Google Scholar], [Publisher]

[14] M.K. Oglah, M.K. Bashir, Y.F. Mustafa, E.T. Mohammed, R. Riyadh, *Syst. Rev. Pharm.,* **2020**, *11*, 717–725. [Google Scholar], [Publisher]

[15] Y.F. Mustafa, E.T. Mohammed, R.R. Khalil, *Egypt. J. Chem.,* **2021**, *64*, 4461–4468. [Crossref], [Google Scholar], [Publisher]

[16] Y.F. Mustafa, N.T. Abdulaziza, M.H. Jasim, *Egypt. J. Chem.,* **2021**, *64*, 1807–1816. [Crossref], [Google Scholar], [Publisher]

[17] Y.F. Mustafa, N.T. Abdulaziz, *NeuroQuantology,* **2021**, *19*, 175–186. [Crossref], [Google Scholar], [Publisher]

[18] M.K. Bashir, Y.F. Mustafa, M.K. Oglah, *Syst. Rev. Pharm.,* **2020**, *11*, 175–187. [Google

[1] The second scientific session of the academic year 2020-2021 on Sunday September 11, 2020.

Scholar], [Publisher]
[19] Y.F. Mustafa, M.K. Bashir, M.K. Oglah, R.R. Khalil, E.T. Mohammed, *NeuroQuantology,* **2021**, *19*, 129–138. [Crossref], [Google Scholar], [Publisher]
[20] A.B. Roomi, G. Widjaja, D. Savitri, A.T. Jalil, Y.F. Mustafa, L. Thangavelu, G. Kazhibayeva, W. Suksatan, S. Chupradit, S. Aravindhan, *J. Nanostructures,* **2021**, *11*, 514-523. [Crossref], [Google Scholar], [Publisher]
[21] H.S. Budi, M.F. Jameel, G. Widjaja, M.S. Alasady, T. Mahmudiono, Y.F. Mustafa, I. Fardeeva, M. Kuznetsova, *Brazilian J. Biol.,* **2022**, *84*, e257070. [Crossref], [Google Scholar], [Publisher]
[22] Y.F. Mustafa, *J. Med. Chem. Sci.,* **2021**, *4*, 612–625. [Crossref], [Google Scholar], [Publisher]
[23] M. Tasior, D. Kim, S. Singha, M. Krzeszewski, K.H. Ahn, D.T. Gryko, *J. Mater. Chem. C,* **2015**, *3*, 1421–1446. [Crossref], [Google Scholar], [Publisher]
[24] H. Lv, P. Tu, Y. Jiang, *Mini-Reviews Med. Chem.,* **2014**, *14*, 603–622. [Crossref], [Google Scholar], [Publisher]
[25] Y.F. Mustafa, S.M. Kasim, B.M. Al-Dabbagh, W. Al-Shakarchi, *Appl. Nanosci.,* **2021**. [Crossref], [Google Scholar], [Publisher]
[26] Y.F. Mustafa, M.K. Bashir, M.K. Oglah, *Syst. Rev. Pharm.,* **2020**, *11*, 598–612. [Google Scholar], [Publisher]
[27] F.A.H. Hussien, M. Keshe, K. Alzobar, J. Merza, A. Karam, *Int. Lett. Chem. Phys. Astron.,* **2016**, *69*, 66–73. [Crossref], [Google Scholar], [Publisher]
[28] Y.F. Mustafa, *Appl. Nanosci.,* **2021**. [Crossref], [Google Scholar], [Publisher]
[29] Y.F. Mustafa, N.A. Mohammed, *Biochem. Cell. Arch.,* **2021**, *21*, 1991–1999. [Google Scholar], [Publisher]
[30] Y.A. Atia, D.O. Bokov, K.R. Zinnatullovich, M.M. Kadhim, W. Suksatan, W.K. Abdelbasset, H.A. Hammoodi, Y.F. Mustafa, Y. Cao, *Mater. Chem. Phys.,* **2022**, *278*, 125664. [Crossref], [Google Scholar], [Publisher]
[31] Y.F. Mustafa, E.T. Mohammed, R.R. Khalil, *Syst. Rev. Pharm.,* **2020**, *11*, 570–576. [Google Scholar], [Publisher]
[32] Y.F. Mustafa, M.K. Oglah, M.K. Bashir, *Syst. Rev. Pharm.,* **2020**, *11*, 482–489. [Google Scholar], [Publisher]
[33] H. Aldewachi, Y.F. Mustafa, R. Najm, F. Ammar, *Syst. Rev. Pharm.,* **2020**, *11*, 289–296. [Google Scholar], [Publisher]
[34] Y.F. Mustafa, R.R. Khalil, E.T. Mohammed, *Egypt. J. Chem.,* **2021**, *64*, 3711–3716. [Crossref], [Google Scholar], [Publisher]
[35] F. Cheng, W. Li, G. Liu, Y. Tang, *Curr. Top. Med. Chem.,* **2013**, *13*, 1273–1289. [Crossref], [Google Scholar], [Publisher]
[36] Y.F. Mustafa, M.K. Oglah, M.K. Bashir, E.T. Mohammed, R.R. Khalil, *Clin. Schizophr. Relat. Psychoses,* **2021**, *15*, 1–6. [Google Scholar], [Publisher]
[37] A.M. Nejres, Y.F. Mustafa, H.S. Aldewachi, *Int. J. Pavement Eng.,* **2022**, *23*, 39–45. [Crossref], [Google Scholar], [Publisher]
[38] A.M. Nejres, H.K. Ali, S.P. Behnam, Y.F. Mustafa, *Syst. Rev. Pharm.,* **2020**, *11*, 726–732. [Google Scholar], [Publisher]
[39] I. Raya, T. Chen, S.H. Pranoto, A. Surendar, A.S. Utyuzh, S. Al-janabi, A.F. Alkaim, N.T. Danh, Y.F. Mustafa, *Mater. Res.,* **2021**, *24*, e20210245. [Crossref], [Google Scholar], [Publisher]
[40] R.L. Freire, M.B. Marques, E.M.D. Souza-Fagundes, R.B.D. Oliveira, R.J. Alves, *Brazilian J. Pharm. Sci.* **2017**, *53*, e15235. [Crossref], [Google Scholar], [Publisher]

How to cite this article: Sara Firas Jasim*, Yasser Fakri Mustafa. New fused-coumarin composites: synthesis, anticancer and antioxidant potentials evaluation. *Eurasian Chemical Communications*, 2022, 4(7), 607-619. **Link:** http://www.echemcom.com/article_147418.html

Copyright © 2022 by SPC (Sami Publishing Company) + is an open access article distributed under the Creative Commons Attribution License(CC BY) license (https://creativecommons.org/licenses/by/4.0/), which permits unrestricted use, distribution, and reproduction in any medium, provided the original work is properly cited.